Supramolecular Hydrogels Hybridized with Single-Walled Carbon Nanotubes

Zhimin Wang and Yongming Chen*

State Key Laboratory of Polymer Physics and Chemistry, Institute of Chemistry, The Chinese Academy of Sciences, Beijing 100080, China

Received January 29, 2007; Revised Manuscript Received March 9, 2007

ABSTRACT: In this study, well-dispersed single-walled carbon nanotubes (SWNTs) were successfully incorporated into a supramolecular hydrogel through combining dual roles of Pluronic copolymer in dispersing SWNTs and forming inclusion complexes with α-cyclodextrin (α-CD). Such hydrogel hybridized with SWNTs was prepared by mixing an aqueous solution of α-CD with an aqueous dispersion of SWNTs stabilized by Pluronic copolymer. The structure and properties of the supramolecular hydrogels were studied in detail by means of a variety of characterization methods. The results obtained from X-ray diffraction (XRD), Raman spectroscopy, differential scanning calorimetry (DSC), and scanning electron microscopy (SEM) showed that the introduction of well-dispersed SWNTs had no obvious influence on the structure and morphology but changed the gelation mechanism comparing with that of the native hydrogel. The resultant hybrid hydrogel retained the basic characters of supramolecular hydrogel, especially the shear-thinning and reversible temperature-responsive properties. It is noteworthy that the introduction of SWNTs accelerated the gel formation obviously, but the ultimate strength of the hybrid hydrogels, characterized by viscosities and storage modulus, declined with the increase of SWNTs.

Introduction

During the past few years great attention has been paid to carbon nanotubes (CNTs) due to their extraordinary mechanical, thermal, and electrical properties.[1] Among them, developing multifunctional nanocomposites based on CNTs combining the characters of organic polymers or other matrix with the unique properties of carbon nanotubes have come forth as an important and active field.[2] However, manipulation and incorporation of CNTs into different matrixes are always problematic due to poor solubility and low dispersibility of CNTs in water or organic solvents.[3] To this respect, much effort has been made on modification of CNTs through covalent or noncovalent strategies to improve their solubility and processability, and much progress has been achieved during past few years.[4]

One of the most exciting applications of carbon nanotubes is in biomedical field.[5] A large number of documents have shown that carbon nanotubes could cross cell membranes easily and deliver peptides, proteins, nucleic acids, and small therapeutic molecules, e.g., anticancer drug, antibacterial, or antiviral agent, into cells.[6] Also, CNTs have been proposed as biosensors for DNA or protein,[7] scaffolds for cell growth,[8] imaging reagents,[9] and near-infrared agents for selective cancer cell destruction.[10] They have also been used as new platforms to detect antibodies associated with human autoimmune diseases with high specificity.[11] Although large numbers of works have been made in biological systems, most of them were conducted in vitro rather than in vivo. How to transport the carbon nanotubes safely into the organisms is a controversial issue. From this viewpoint, new approaches to stabilize and deliver CNTs, like the injectable supramolecular hydrogels,[12] are urgently needed for this issue.

Smart supramolecular hydrogels have attracted much attention due to their potential applications in the fields of drug delivery and release,[12b,13] biological assay or sensors,[14,15] and biomedical or tissue engineering.[16] Cyclodextrins (CDs) are cyclic oligosaccharides with D-(+)-glucose as the repeating unit coupled by α-1,4-linkages. α-, *β*-, and *γ*-CDs are commonly available forms which consist of 6, 7, and 8 glucose units, respectively.[17] Thanks to the existence of hydrophobic cavity, CDs have been extensively studied as host molecules in supramolecular chemistry because they can include different guest molecules ranging from low molecular weight organic or inorganic compounds to polymers.[18] Following the first discovery by Harada et al. that poly(ethylene oxide) (PEO) can form inclusion complexes with α-CDs,[19] a great of effort has been made to explore the inclusion complexation between different polymers and CDs.[20] Pluronic block copolymer, poly(ethylene oxide)-*block*-poly(propylene oxide)-*block*-poly(ethylene oxide) triblock copolymer (PEO-*b*-PPO-*b*-PEO), could form supramolecular hydrogels when the PEO blocks being threaded with α-CD rings in aqueous solution.[21] It is noteworthy that such hydrogel may be transformed into a sol when stimulated by temperature or shear force and this process is reversible. Coincidentally, apart from the formation of supramolecular hydrogels, Pluronic triblock copolymers could also disperse pristine SWNT in water.[22] Thus, integrating the dual roles of Pluronic copolymer in dispersing CNTs and in forming hydrogels with α-CD, one may fabricate a novel supramolecular hydrogel nanocomposite containing well-dispersed carbon nanotubes. The resulting nanocomposite, combined the useful properties of hydrogels with SWNTs, is believed to possess some outstanding properties for biomedical applications. For instance, this kind of supramolecular hybrid hydrogel can be used to transport the SWNTs or therapy drugs carried by SWNTs or hyrogels.

So far, few researches have been reported on the gel formation with or in presence of CNTs.[23] Particularly, the hydrogels hybridized with CNTs are sought after for bio-inspired application. Li et al.[24] have reported a novel hybrid gelatin hydrogel with multiwalled carbon nanotubes (MWNTs), where the MWNTs can be taken as an additive to enhance the mechanical property of the hydrogel. Asai et al.[25] have also reported the preparation of a novel hydrogel with dispersed SWNTs based on sugar-based gelators bearing an azonaphthol moiety by the

* Corresponding author: E-mail: ymchen@iccas.ac.cn.

10.1021/ma0702593 CCC: $37.00
Published on Web 04/04/2007

interaction between the π-group in the gelator and the surface of SWNTs. However, as far as we knew, there is no report addressed the incorporation of CNTs into polymer hydrogel systems. Hence, we sought to examine whether incorporation of SWNTs into polymer supramolecular hydrogel is feasible and, if so, how the structure, morphology, and properties of the resultant hybrid hydrogel are influenced upon incorporation of SWNTs.

Herein, we report a facile strategy to introduce SWNTs into the supramolecular hydrogel formed by host−guest interaction. Because of the dual functions of Pluronic copolymer mentioned above, SWNTs could be well dispersed individually or thin bundled into the hydrogel matrix in situ. The resulted hybrid hydrogel retained the basic characters of supramolecular hydrogel and pristine SWNTs, especially the shear-thinning and thermal stimulus responsive properties, which are important in drug delivery and controlled release. Also, it was found that the presence of SWNTs might accelerate the gel formation but weaken the gel strength compared with the native hydrogel.

Experimental Section

Materials and Methods. Pluronic copolymer (Aldrich, M_n = 13 440, M_w/M_n = 1.02, PEO 82.5 wt %), α-CD (Wacker Chemie AG, AP. grade), and pristine single-walled carbon nanotubes (Timesnano, prepared by chemical vapor deposition method, 90 wt % pure SWNTs, 1−2 nm in diameter and several micrometers in length) were used without further purification.

To disperse SWNTs in Pluronic aqueous solution, 200 mg of Pluronic copolymer and 20 mg of SWNTs were charged into a 50 mL flask with 20 mL of deionized water, and the mixture was sonicated for 30 min, followed by centrifugation at 8000 rpm for 60 min, resulting in a homogeneously black solution. To estimate the exact concentration of SWNTs and Pluronic copolymer in the solution, the precipitate was collected and dried under vacuum for 24 h; the amounts of SWNTs and polymer were determined by thermogravimetric analysis (TGA).

The SWNT solution prepared above was used for preparing the hybrid hydrogels with different amounts of SWNTs. The details were described as follows: First, quantitative α-CD was dissolved in water to form a transparent solution. Then the solutions of SWNT and α-CD were mixed together, and the ultimate concentration of α-CD in the mixture was fixed to be of 90 mg/mL. The concentration of Pluronic copolymer was kept at 10 mg/mL by accession of some free Pluronic copolymer in order to make the ratio of α-CD to EO units to be 1:2. The mixed solutions containing different amounts of SWNTs were kept still for certain time for further characterizations. Three hydrogel samples containing 0.01, 0.05, and 0.2 wt % SWNTs were prepared for comparison. The native hydrogel without SWNTs was prepared under the same condition for comparison.

Measurements. Transmit electron microscopy (TEM) observations were conducted on a JEM-100 electron microscope at an acceleration voltage of 100 kV. The sample was prepared though depositing a drop of the dispersion solution of Pluronic-assisted dispersed SWNTs on a TEM grid (300 mesh Cu grid) coated with Formvar and carbon film. For SEM observations, the specimens were freeze-dried under vacuum overnight. The dried specimens were ground to fine powder and placed carefully on conducting glue and then coated with gold vapor to make them conducting and analyzed on a JSM 6700F SEM operated at 5.0 kV. DSC measurements were performed under nitrogen at a flow rate of 30 mL/min on a Perkin-Elmer Diamond differential scanning calorimeter. Each sample was heated from −20 to 160 °C at a heating rate of 10 °C/min and scanned two times to erase thermal history. XRD patterns of the complexes were recorded on a Rigabu D/max 2500 X-ray powder diffractometer with Cu Kα (1.541 Å) radiation (40 kV, 40 mA). Powder samples were mounted on a sample holder and scanned with a step size of 0.01° between 2θ = 3° and 50°. The measurements of Raman spectra were performed with a JY-HR800 (France) Raman apparatus, using a 532 nm laser beam with a laser power of 5 mW and a detector data acquisition time of 100 s. The gels formation were traced by the changes of viscosity of the sols, using a Brookfield HADV-iii+ digital viscometer coupled with a small sample adapter SSA 15/7R and a temperature controlling unit. For measuring the rheological behaviors of the hydrogels, a TA-AR2000 rheometer with parallel-plate geometry (CP 25-2) was used. The gap distance between the two plates was fixed at 1 mm. The specimens were scooped on the plate of the rheometer for conducting. The steady flow behaviors were performed at shear rate range from 0.01 to 50 s^{-1}. A stress−amplitude sweep experiment was performed at a constant oscillation frequency of 1 Hz for the strain range 0.01−10 at 30 °C. Oscillating strain was fixed at 0.1 for all the dynamic tests. The rheometer had a built-in computer which converted the torque measurements into either G' (storage modulus) or G'' (loss modulus) in oscillatory shear experiments.

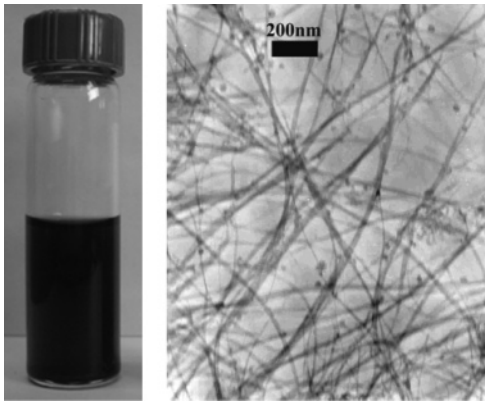

Figure 1. Optical photo (left) and TEM image (right) of the dispersion of SWNTs in water by Pluronic copolymer.

Results and Discussion

As depicted in the literature,[22] Pluronic copolymer could effectively disperse SWNTs by sonicating the as-prepared SWNTs in aqueous solution. To separate those undissolved SWNT bundles and impurities, the solution was supercentrifuged for 60 min and the precipitation was collected and dried for TGA (Figure S1 in Supporting Information). Thus, the exact concentrations of SWNTs and Pluronic in the solution could be determined to be 0.2 and 9 mg/mL based on the amounts of feed and precipitation. As shown in Figure 1, macroscopically homogeneous dispersion of SWNTs could be obtained, and the exfoliated individual or thin bundles of SWNTs can be clearly observed from the TEM image. This dispersion of SWNTs could be diluted to form a steady and transparent solution, which can last for at least 6 months without precipitation occurring.

When α-CD solution was added, the processes of gel formation recorded by an optical camera are shown in Figure 2. The sol system with well-dispersed SWNTs formed an invertible hydrogel in about 25 min, while the native sol system remained ambulatory. After ca. 60 min, both two systems can form invertible hydrogels. These results indicate that the addition of well-dispersed SWNTs in the sol system can obviously accelerate the formation of hydrogel.

Similar results were obtained through tracing the change of viscosity during the gel formation by using a digital viscometer. As shown in Figure 3, the viscosity of the sol system containing well-dispersed SWNTs reveals a dramatic increase at ca. 25 min, when the hydrogel could be invertible. However, the native sol system exhibited a slower increase of viscosity during the initiatory 70 min and the gel could not be invertible until 60 min, when the viscosity reached 300 cP. This agrees with the results observed in Figure 2.

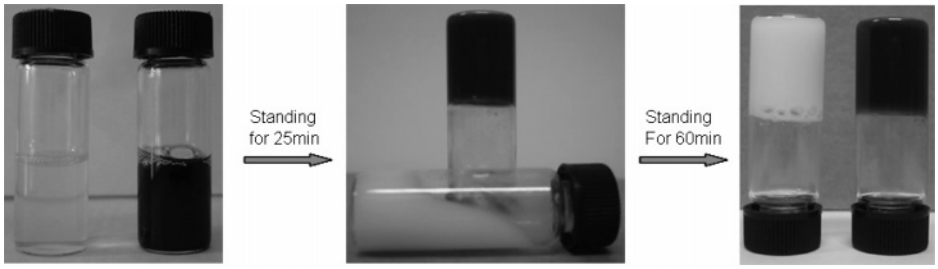

Figure 2. Evolvement of the hybrid supramolecular hydrogels formation traced by a digital camera comparing with the native hydrogel.

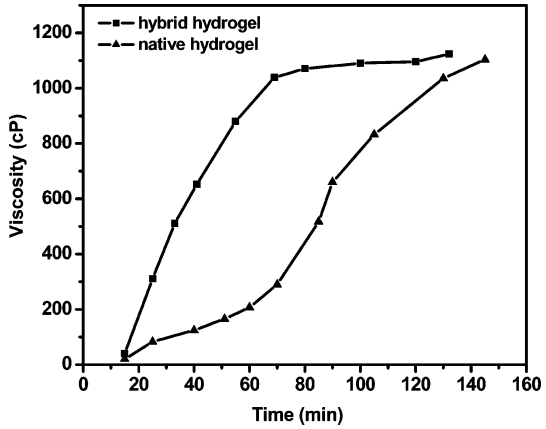

Figure 3. Comparison of the kinetics of supramolecular hydrogel formation with and without SWNTs.

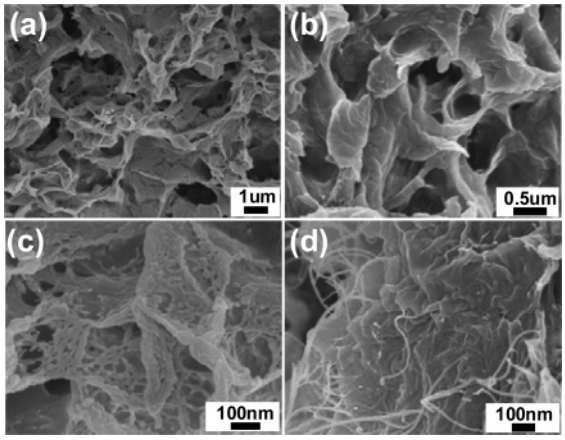

Figure 4. SEM images of morphologies of the supramolecular hydrogels and dispersing state of SWNTs: (a) native hydrogel and (b) hybrid hydrogel at low magnification; (c) native hydrogel and (d) hybrid hydrogel at high magnification.

To determine the morphology of the hydrogels and the dispersion of SWNTs, the hydrogels were freeze-dried and observed by SEM. As shown in Figure 4, at the lower magnification, both the native and the hybrid hydrogels exhibited a loose spongelike structure, indicating the leakage of the trapped water during freeze-drying. At the higher magnification, well-dispersed individual or thin bundled SWNTs could be identified in the hybrid hydrogel. Comparing the native hydrogel with the hybrid hydrogel carefully at the higher magnification, one can observe that the surface of the hybrid hydrogel is relatively smooth, while the native hydrogel looks a bit coarse with plentiful undulant pimples. This difference may be caused by the interaction of the PPO block with SWNTs, which limited the movement and micellization of PPO block and resulted in a slight change of the morphology.

To examine the effect of SWNTs on the structure of the hydrogel, Raman spectroscopy was used to compare the

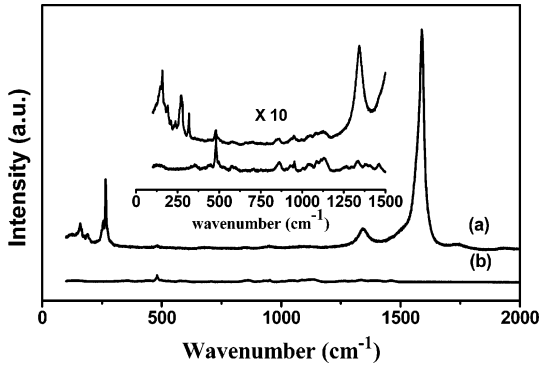

Figure 5. Comparison of the hybrid (a) and native (b) hydrogels by Raman spectroscope; the inset shows the local magnified view.

difference between the native and hybrid hydrogels with the freeze-dried samples; also, the existence and the dispersing state of the SWNTs in the hybrid hydrogel could be confirmed. As shown in Figure 5a, the characteristic D-band at 1344 cm^{-1} and G-band at 1590 cm^{-1} of SWNTs, corresponding to the disorder mode and tangential mode, respectively, could be clearly observed, indicating the existence of SWNTs in the hybrid hydrogel. In addition, the D-band was weaker relative to the G-band, indicating the pristine character of the as-prepared SWNTs. A prominent feature in the Raman spectrum of SWNTs is the radial breathing mode in the region of 160−300 cm^{-1} associated with a symmetric movement of all carbon atoms in the radial direction. The frequency and modal distribution of the radial breathing modes depend primarily on the diameter and chirality of the nanotubes and whether the nanotubes directly contact on another in bundles.[26] Previously, Rao et al. have established a linear dependence of the breathing mode frequency on the inverse of the tube diameter.[27] Later, this has been amended to take into account the intertubule interaction within a bundle as shown in the following equation:[28]

$$\omega_r = \frac{223.75\ \text{nm}\cdot\text{cm}^{-1}}{d\ (\text{nm})} + 14\ \text{cm}^{-1}$$

where ω_r is the radial breathing mode frequency, d is the diameter, and the 14 cm^{-1} correction represents a d-independent approximation to the effect of the weak intertubule interaction. Using this relationship, we can calculate the diameter range of SWNTs in the present hybrid hydrogel. From the relative intensity of the peaks, we can also determine the ratios of SWNTs with different diameters. From the magnified image of the Raman spectrum (see Figure S2 in Supporting Information), five weak peaks could be found at 159, 165, 175, 185, and 190 cm^{-1}, which were from the raw SWNT powder.[26] Three new and strong peaks at 248, 255, and 265 cm^{-1}, corresponding to the individual or thin-bundled SWNTs with diameter ~0.9 nm, demonstrated well dispersion of SWNTs in the hybrid hydrogel. The inset in Figure 5 shows the local magnification

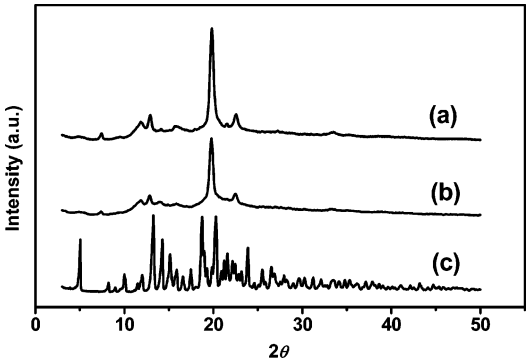

Figure 6. XRD patterns of (a) native hydrogel, (b) hybrid hydrogel, and (c) pure α-CD.

which may help the comparison of the two hydrogels. Apart from the stronger signals from SWNTs in hybrid hydrogel, there is almost no difference in structure between the hybrid hydrogel and the native hydrogel.

To confirm that the gel formation was caused by inclusion interaction between PEO blocks of the Pluronic copolymers and α-CD, wide-angle X-ray diffractions were conducted with the freeze-dried samples. As shown in Figure 6, compared to the pure α-CD, a characteristic peak at $2\theta = 19.4°$ ($d = 4.57$ Å), representing the channel-type structure of α-CD and PEO complex, was observed in the diffractograms of the two hydrogels.[21] However, the patterns of the hybrid hydrogel were nearly the same with that of the native hydrogel. This result indicates that the addition of SWNTs had no effect on the inclusion interaction between PEO block and α-CD, and the driving force for the gelation in this hybrid system is still the inclusion complexation.

To further examine the structural character of the hydrogels, the DSC measurements of Pluronic copolymer, α-CD, native hydrogel, and hybrid hydrogel with the freeze-dried samples were performed (see Figure S3 in Supporting Information). For Pluronic copolymer, a distinct endothermal peak was observed which corresponded to the melting temperature of the crystallizable PEO segments. However, the traces of native hydrogel and hybrid hydrogel showed similarly featureless curves, demonstrating that the PEO side chains were threaded by α-CDs.

The results obtained above clearly indicated that the incorporation of SWNTs into the supramolecular hydrogels did not have an obvious impact on the structure of the supramolecular hydrogel compared to the native hydrogel. This finding prompted us to investigate whether the rheological behaviors of the hybrid hydrogels would be influenced by incorporation of SWNTs. Such studies could give information about the flow behavior and the rigidity of the hydrogels. Accordingly, the steady flow and the dynamic rheological behaviors of the native hydrogel and the hybrid hydrogels were measured. As shown in Figure 7, both the hydrogels exhibited shear-thinning behavior, which is a typical character of supramolecular hydrogels.[12] A notable fact could be seen that the incorporation of SWNTs into the hydrogel resulted in a distinct decline of viscosity compared to the native hydrogel. To further explore the influence of SWNTs on the viscosity and the ultimate intensity of the hybrid hydrogel, three samples with different SWNT concentrations were employed for rheological characterization after the samples were kept still for 1 week. The steady flow results showed a visible decline of viscosity with the increase of SWNTs; the corresponding results are shown in Figure S4 (in Supporting Information).

Small-deformation oscillatory measurements were used to evaluate the viscoelastic behavior of the two hydrogels and study

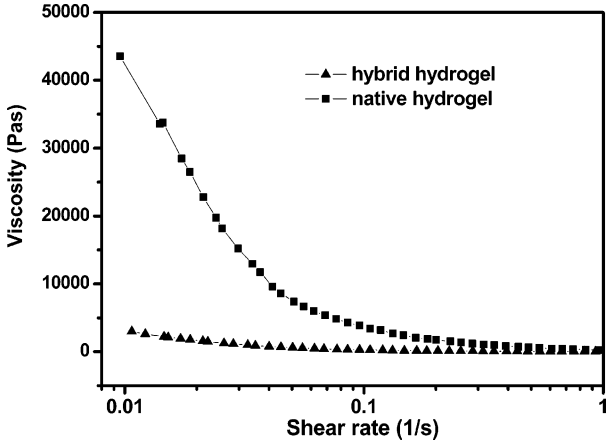

Figure 7. Steady rheological behaviors of the native and hybrid hydrogels.

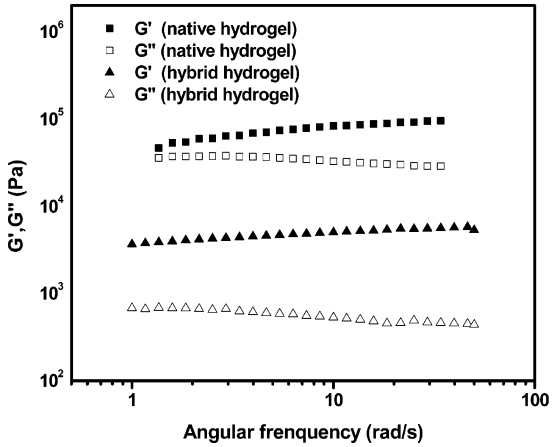

Figure 8. Dynamic rheological behaviors of the native and hybrid hydrogels.

the effects of SWNTs on the hydrogel strength. Figure 8 presents the storage modulus (G') and loss modulus (G'') evolutions of the hybrid hydrogel containing 0.2 wt % SWNTs as a function of frequency compared with the native hydrogel. The G' values of the two hydrogels exhibit a substantial elastic response, which are greater than the loss modulus G'' over the entire range of frequency, indicating the formation of strong and rigid hydrogels. However, similar to the steady flow model, the incorporation of SWNTs resulted in distinct decline of storage modulus, loss modulus, and complex viscosity. More details on the influence of SWNT contents on the dynamic rheological behaviors of the hydrogels are given in Figure S5-6 (in Supporting Information).

It is known that CNTs have been expected as a strengthening agent for developing high-performance polymer nanocomposites. However, in this study we found that the addition of SWNTs accelerated the gelation process obviously during the initiatory stage but caused the decline of the ultimate strength of the hybrid hydrogels. These results can be explained from the mechanisms of hydrogel formation and SWNTs dispersion by Pluronic copolymer. As reported by Li et al.,[21] the driving force for the gelation of Pluronic and α-CD solutions is a combination of the crystallization of inclusion columns between α-CD and PEO blocks and the micellization of the PPO blocks; i.e., there are two types of physical cross-linking points. Moreover, it was reported that the dispersion of pristine SWNTs by Pluronic copolymer is based on the hydrophobic interaction in water, where PPO blocks adsorb onto the hydrophobic surface of the SWNTs and PEO blocks form a corona to dissolve the

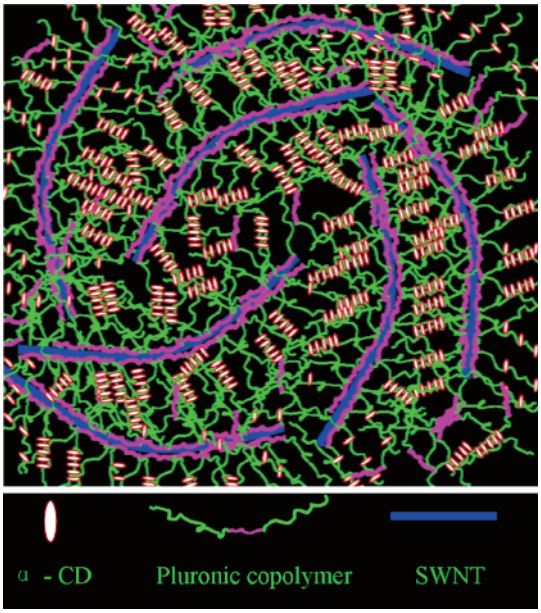

Figure 9. Proposed structure of the supramolecular hydrogel in the presence of well-dispersed SWNTs.

pristine SWNTs.[22] Since the cross-linking networks formed by inclusion complexation were the same for the native and hybrid gel systems, the difference in gelation process and ultimate strength should be related with the micellization extents of the PPO segments in the two systems. In the hybrid sol system, the PEO blocks had been preorganized along the SWNTs before addition of α-CDs. Once α-CDs were threaded onto the PEO blocks, the corresponding cross-linking occurred and the hydrogel formed simultaneously; this could be a fast process. Owing to the adsorption, the micellization of PPO blocks was restrained and, as a result, the density of cross-linking points was decreased. Therefore, the ultimate strength of the hybrid hydrogel declined. A possible structure of the hybrid hydrogel was proposed and shown in Figure 9. Whereas, for the native sol system, the micellization of the PPO blocks would be important, although this process might be slower than that of the inclusion complexation. Further micellization of PPO blocks would increase the density of cross-linking points, which would improve the ultimate intensity of the hydrogel.

Conclusion

This work demonstrated a simple and effective method to hybridize the well-dispersed SWNTs into a supramolecular hydrogel by utilizing the dual roles of Pluronic copolymer in dispersing SWNTs and forming supramolecular hydrogel with α-CDs. The resultant hybrid hydrogels retained the basic characters of supramolecular hydrogel and pristine SWNTs, especially the shear-thinning property, which is very important in drug delivery and controlled release. The process of hydrogel formation was accelerated in the presence of SWNTs. However, the ultimate viscosity and strength of the hybrid hydrogels declined compared to that of the native hydrogel. Furthermore, the hybrid supramolecular hydrogel can be transformed into a sol by increasing temperature, and this process is reversible. Thus, this kind of hybrid hydrogel may find useful applications in biological or biomedical fields not only due to the important application of supramolecular hydrogel but also due to the unique properties of SWNTs.

Acknowledgment. Financial support from the 973 program of MOST (G2003CB615605) and National Science Foundation of China (20534010 and 20625412) is greatly acknowledged.

Supporting Information Available: Thermogravimetric analysis, magnified view of radial breathing model, DSC traces, and rheological behavior characterizations. This material is available free of charge via the Internet at http://pubs.acs.org.

References and Notes

(1) Dresselhaus, M. S.; Dresselhaus, G.; Avouris, P. *Carbon Nanotubes: synthesis, structure, properties and applications*; Springer-Verlag Press: Heidelberg, 2001.
(2) (a) Thostenson, E. T.; Chou, T.-W. *Adv. Mater.* **2006**, *18*, 2837−2841. (b) Wang, X. T.; Padture, N. P.; Tanaka, H. *Nat. Mater.* **2004**, *3*, 539−544. (c) Fennimore, A. M.; Yuzvinsky, T. D.; Han, W. Q.; Fuhrer, M. S.; Cumings, J.; Zettl, A. *Nature (London)* **2003**, *424*, 408−410.
(3) (a) Calvert, P. *Nature (London)* **1999**, *399*, 210−211. (b) Bahr, J. L.; Mickelson, E. T.; Bronikowski, M. J.; Smalley, R. E.; Tour, J. M. *Chem. Commun.* **2001**, 193−194. (c) Lee, H.-J.; Oh, S.-J.; Choi, J.-Y.; Kim, J. W.; Han, J.; Tan, L.-S.; Baek, J.-B. *Chem. Mater.* **2005**, *17*, 5057−5064. (d) Cadek, M.; Coleman, J. N.; Ryan, K. P.; Nicolosi, V.; Bister, G.; Fonseca, A.; Nagy, J. B.; Szostak, K.; Beguin, F.; Blau, W. J. *Nano Lett.* **2004**, *4*, 353−356.
(4) (a) Banerjee, S.; Hemraj-Benny, T.; Wong, S. S. *Adv. Mater.* **2005**, *17*, 17−29. (b) Georgakilas, V.; Kordatos, K.; Prato, M.; Guldi, D. M.; Holzinger, M.; Hirsch, A. *J. Am. Chem. Soc.* **2002**, *124*, 760−761. (c) Niyogi, S.; Hamon, M. A.; Hu, H.; Zhao, B.; Bhowmik, P.; Sen, R.; Itkis, M. E.; Haddon, R. C. *Acc. Chem. Res.* **2002**, *35*, 1105−1113.
(5) (a) Chen, X.; Lee, G. S.; Zettl, A.; Bertozzi, C. R. *Angew. Chem., Int. Ed.* **2004**, *43*, 6112−6116. (b) Williams, K. A.; Veenhuizen, P. T. M.; de la Torre, B. G.; Eritja, R.; Dekker, C. *Nature (London)* **2002**, *420*, 761−761.
(6) (a) Kam, N. W. S.; Dai, H. *J. Am. Chem. Soc.* **2005**, *127*, 6021−6026. (b) Singh, R.; Pantarotto, D.; McCarthy, D.; Chaloin, O.; Hoebeke, J.; Partidos, C. D.; Briand, J.-P.; Prato, M.; Bianco, A.; Kostarelos, K. *J. Am. Chem. Soc.* **2005**, *127*, 4388−4396. (c) Li, Q.; Moore, J. M.; Huang, G.; Mount, A. S.; Rao, A. M.; Larcom, L. L.; Ke, P. C. *Nano Lett.* **2004**, *4*, 2473−2477.
(7) (a) Li, J.; Ng, H. T.; Cassell, A.; Fan, W.; Chen, H.; Ye, Q.; Koehne, J.; Han, J.; Meyyappan, M. *Nano Lett.* **2003**, *3*, 597−602. (b) Gooding, J. J.; Wibowo, R.; Liu, J. Q.; Yang, W. R.; Losic, D.; Orbons, S.; Mearns, F. J.; Shapter, J. G.; Hibbert, D. B. *J. Am. Chem. Soc.* **2003**, *125*, 9006−9007. (c) Wang, J.; Liu G.; Jan, M. R. *J. Am. Chem. Soc.* **2004**, *126*, 3010−3011.
(8) (a) Hu, H.; Ni, Y.; Montana, V.; Haddon, R. C.; Parpura, V. *Nano Lett.* **2004**, *4*, 507−511. (b) McKenzie, J. L.; Waid, M. C.; Shi, R.; Webster, T. J. *Biomaterials* **2004**, *25*, 1309−1317.
(9) Cherukuri, P.; Bachilo, S. M.; Litovsky, S. H.; Weisman, R. B. *J. Am. Chem. Soc.* **2004**, *126*, 15638−15639.
(10) Kam, N. W. S.; O'Connell, M.; Wisdom, J. A.; Dai, H. J. *Proc. Natl Acad. Sci. U.S.A.* **2005**, *102*, 11600−11605.
(11) Chen, R. J.; Bangsaruntip, S.; Drouvalakis, K. A.; Kam, N. W.; Shim, M.; Li, Y.; Kim, W.; Utz, P. J.; Dai, H. J. *Proc. Natl. Acad. Sci. U.S.A.* **2003**, *100*, 4984−4989.
(12) (a) Chen, G.; Hoffman, A. S. *Nature (London)* **1995**, *373*, 49−52. (b) Li, J.; Ni, X. P.; Leong, K. W. *J. Biomed. Mater. Res. A* **2003**, *65A*, 196−202.
(13) Hoffman, A. S. *Adv. Drug Delivery Rev.* **2002**, *43*, 3−12.
(14) Yamaguchi, S.; Yoshimura, I.; Kohira, T.; Tamaru, S.; Hamachi, I. *J. Am. Chem. Soc.* **2005**, *127*, 11835−11841.
(15) Kiyonaka, S.; Sada, K.; Yoshimura, I.; Shinkai, S.; Kato, N.; Hamachi, I. *Nat. Mater.* **2004**, *3*, 58−64.
(16) Lee, K. Y.; Mooney, D. J. *Chem. Rev.* **2001**, *101*, 1869−1880.
(17) (a) Szejtli, J. *Chem. Rev.* **1998**, *98*, 1743−1754. (b) Lipkowitz, K. B. *Chem. Rev.* **1998**, *98*, 1829−1874.
(18) (a) Wenz, G. *Angew. Chem., Int. Ed. Engl.* **1994**, *33*, 803−822. (b) Nepogodiev, S. A.; Stoddart, J. F. *Chem. Rev.* **1998**, *98*, 1959−1976.
(19) Harada, A.; Kamachi, M. *Macromolecules* **1990**, *23*, 2821−2823.
(20) (a) Nepogodiev, S. A.; Stoddart, J. F. *Chem. Rev.* **1998**, *98*, 1959−1976. (b) He, L.; Huang, J.; Chen, Y.; Xu, X.; Liu, L. *Macromolecules* **2005**, *38*, 3845−3851. (c) Sabadini, E.; Cosgrove, T. *Langmuir* **2003**, *19*, 9680−9683.
(21) Li, J.; Li, X.; Zhou, Z.; Ni, X.; Leong, K. W. *Macromolecules* **2001**, *34*, 7236−7237.
(22) (a) Moore, V. C.; Strano, M. S.; Haroz, E. H.; Schmidt, J.; Talmon, Y.; Hauge, R. H.; Smalley, R. E. *Nano Lett.* **2003**, *3*, 1379−1382. (b)

Shvartzman-Cohen, R.; Levi-Kalisman, Y.; Nativ-Roth, E.; Yerushalmi-Rozen, R. *Langmuir* **2004**, *20*, 6085−6088.
(23) (a) Kovtyukhova, N. I.; Mallouk, T. E.; Pan, L.; Dickey, E. C. *J. Am. Chem. Soc.* **2003**, *125*, 9761−9769. (b) Sabba, Y.; Thomas, E. L. *Macromolecules* **2004**, *37*, 4815−4820. (c) Chen, J.; Xue, C. H.; Ramasubramaniam, R.; Liu, H. Y. *Carbon* **2006**, *44*, 2142−146. (d) Fukushima, T.; Kosaka, A.; Ishimura, Y.; Yamamoto, T.; Takigawa, T.; Ishii, N.; Aida, T. *Science* **2003**, *300*, 2072−2074.
(24) Li, H.; Wang, D. Q.; Chen, H. L.; Liu, B. L.; Gao, L. Z. *Macromol. Biosci.* **2003**, *3*, 720−724.
(25) Asai, M.; Sugiyasu, K.; Fujita, N.; Shinkai, S. *Chem. Lett.* **2004**, *33*, 120−121.
(26) (a) Dieckmann, G. R.; Dalton, A. B.; Johnson, P. A.; Razal, J.; Chen, J.; Giordano, G. M.; Munoz, E.; Musselman, I. H.; Baughman, R. H.; Draper, R. K. *J. Am. Chem. Soc.* **2003**, *125*, 1770−1777. (b) Hartschuh, A.; Sanchez, E. J.; Xie, X. S.; Novotny, L. *Phys. Rev. Lett.* **2003**, *90*, 095503−095506. (c) Su, Z. D.; Leung, T.; Honek, J. F. *J. Phys. Chem. B* **2006**, *110*, 23623−23627.
(27) Rao, A. M.; Bandow, S.; Richter, E.; Eklund, P. C. *Thin Solid Films* **1998**, *331*, 141−147.
(28) Venkateswaran, U. D.; Rao, A. M.; Richter, E.; Menon, M.; Rinzler, A.; Smalley, R. E.; Eklund, P. C. *Phys. Rev. B* **1999**, *59*, 10928−10934.

MA0702593